

Angiogenesis of renal cell carcinoma: perfusion CT findings

Yan Chen,¹ Jin Zhang,¹ Jingrui Dai,¹ Xiaoli Feng,² Haizhen Lu,² Chunwu Zhou¹

¹Department of Diagnostic Radiology, Cancer Hospital and Institute, Chinese Academy of Medical Sciences and Peking Union Medical College, Beijing, China

²Department of Pathology, Cancer Hospital and Institute, Chinese Academy of Medical Sciences and Peking Union Medical College, Beijing, China

Abstract

Objective: To observe the perfusion CT findings of renal cell carcinoma (RCC) and prospectively correlate perfusion CT parameters with tumor MVD and VEGF expression.

Methods: Dynamic contrast-enhanced multislice spiral CT was performed prospectively in 73 cases with histologically proven RCC (65 clear cell, 3 papillary, and 5 chromophobe). Blood flow (BF), blood volume (BV), mean transit time (MTT), and permeability surface-area product (PS) of RCC and normal renal cortex were measured, respectively. The tumor MVD count and VEGF expression level were determined by immunohistochemistry with specific monoclonal antibodies.

Results: There was significant difference between BF, BV, MTT, and PS of normal renal cortex (454.32 ± 110.90 mL/min/100 g, 23.53 ± 5.71 mL/100 g, 3.62 ± 1.38 s, 63.95 ± 18.85 mL/min/100 g) and RCC (261.96 ± 175.86 mL/min/100 g, 17.17 ± 8.34 mL/100 g, 7.08 ± 3.42 s, 25.07 ± 13.20 mL/min/100 g) ($P < 0.01$). BF and BV among RCC histologic subtypes were significantly different ($P < 0.05$), MTT and PS were not ($P > 0.05$). MVD (42.29 ± 21.00) of RCC is positively correlated with BF, BV, and PS ($P < 0.01$), not with MTT ($P > 0.05$). No relationship was found between the expression levels of VEGF and any perfusion CT parameter.

Conclusions: Perfusion CT is a feasible technique to assess tissue perfusion in patients with RCC. BV, BF, and PS correlate positively with MVD and may reflect angiogenesis of RCC.

Key words: Renal cell carcinoma—Tomography—X-ray computed—Perfusion imaging—Tumor angiogenesis—Microvascular density—Vascular endothelial growth factor

Renal cell carcinoma (RCC) is the most common malignant tumor of kidney; most of RCC are hyper-vascular. Angiogenesis plays an important role in the growth and spread of renal cell carcinoma. The study of tumor angiogenesis is currently a leading theme in oncology, and many new drugs targeting the tumor angiogenesis process are under development. There is growing need for rapid and effective biomarkers to monitor clinical response [1].

But it is intricate to quantify angiogenesis because it is a dynamic process. To date, microvascular density (MVD) has been used as the gold standard method to quantify angiogenesis. And VEGF, which is regarded as the more effective angiogenic growth factor, has been used to evaluate the tumor angiogenesis too [2]. But these immunohistochemistry techniques have several limitations: they need to be standardized, require some type of tissue sampling such as a biopsy, cannot be performed repeatedly, and do not explore the entire tumor volume, which can lead to errors due to the heterogeneity of malignant tumors [1].

Therefore, the development of functional imaging techniques to noninvasively quantify the microcirculation over an entire tumor is very promising. As an appropriate noninvasive technique for assessment of angiogenesis, perfusion CT is becoming widely used for the diagnosis of cancers and for the monitoring of tumor's response to therapy. Many investigators have shown that perfusion CT provides an in vivo marker of angiogenesis. Positive correlations between CT parameters and immunohistologic measures, such as microvessel density, have been reported in studies of lung, colorectal and pancreatic tumor [3–5]. However, to our knowledge, there has been no evidence that quantitative parameters such as blood flow (BF), blood volume (BV), or permeability surface-area product (PS) reflect angiogenesis in renal cell carcinoma.

Thus, the aim of our study was to prospectively correlate perfusion CT parameters of renal cell carcinoma with tumor MVD and VEGF expression assessed by using immunohistochemistry techniques, and determine the value of perfusion CT for renal cell carcinoma angiogenesis.

Materials and methods

Patients

From March 2005 to May 2007, kidney dynamic contrast-enhanced CT was performed in 127 patients suspected of renal tumor at our department. Of all, 73 cases of RCC (65 clear cell, 3 papillary, and 5 chromophobe) were confirmed by pathology and underwent surgical resection. This group comprised 50 men and 23 women with a mean age of 50 years (range 24–74 years). The median diameter of the tumor at CT examination was 45 mm (range 15–100 mm). Tumors appeared as homogeneous solid masses in 10 (14%) of 73 cases. Cystic components were found in 63 (86%) of 73 cases, and calcification was not found in any case. None of the examined patients received neoadjuvant treatment before CT examination or surgery. The study was designed in a prospective manner and was approved by the Institutional Review Board of Cancer Hospital, and informed consent was obtained from each participant before the study.

CT technique

All patients were examined with an 8-detector or a 16-detector CT scanner (LightSpeed Ultra, LightSpeed Pro16; GE Healthcare Technologies). A compression band was placed across the abdomen to minimize abdominal wall movement. Patients were trained to hold breathing or breathe slightly during the examination to minimize motion artifacts.

An unenhanced abdominal multislice CT examination (section reconstruction, 5 mm; section interval, 5 mm; 120 kV; 60 mAs; field of view, 36 cm; and 512 × 512-mm matrix) was performed initially to locate the renal tumor.

Supervising radiologists (including Y.C., 6–14 years experience in body CT) selected a perfusion CT volume which was centered on the renal tumor. The greatest dimension plane of the renal tumor with solid component was considered to be the best.

For dynamic perfusion CT imaging, a pump injector (Stellant, Medrad, USA) was used to inject 50 mL of nonionic contrast medium (Optiray 320, Tyco Healthcare, Canada) intravenously at a rate of 4 mL/s. Four contiguous sections, each collimated to 5 mm, were obtained at 1-s intervals by using a cine mode acquisition (120 kV, 51 mAs, 36-cm scanning field of view, 512 × 512-mm matrix). Scanning was initiated 10 s after

the intravenous injection began. It continued for a total of 50 s.

The diagnostic CT scan was performed a few days (range 1–4 days) before perfusion CT examination to determine the local and distant stages of the tumor. Dual phase renal multislice CT was performed at 25–35 s and at 80–90 s, respectively, after the initiation of intravenous injection (volume, 2 mL/kg of body weight; rate, 3 mL/s). The following scanning parameters were used: section reconstruction, 5.0 mm; section interval, 5.0 mm; 120 kV; 68 mAs; field of view for corticomedullary phase, 36 cm; field of view for nephrographic phase, 50 cm; and 512 × 512-mm matrix.

Imaging data analysis

All perfusion CT scanning data were transferred to the workstation (Advantage Windows 4.2; GE Healthcare Technologies) and processed by a radiologist (Y.C., 14 years experience in body CT and 4 years experience in perfusion CT) with perfusion software (Kidney Protocol, Perfusion 3.0; GE Healthcare Technologies).

A representative 5-mm tumor section was selected. To optimize visualization of the soft tissue, a processing threshold of between –30 and 400 HU was chosen. An arterial input was defined within the abdominal aorta by using a mouse to place a circular region of interest (ROI). ROIs of renal tumor, normal renal cortex (affected kidney or opposite kidney) were defined manually, respectively. We took care to ensure that the tumor ROI remained within the tumor boundary and to exclude the necrosis, cyst, hemorrhage and calcification component. A tissue time-enhancement curve and the four perfusion parameters (BF, BV, MTT, and PS) were derived by software automatically for selected ROIs. And parametric maps were generated, with each pixel representing a parameter value (Fig. 1). ROI values for the four perfusion CT parameters were recorded for each patient.

Immunohistochemical staining and quantification of histologic parameters

All patients underwent surgical resection within 2 weeks after perfusion CT examination. In addition to routine tissue samples for pathologic diagnosis, additional tissue blocks from each tumor were acquired for additional immunohistochemical staining by the pathologist. Discussing with the radiologist who supervised the perfusion CT study, the pathologist took care to ensure sampling at a tumor level corresponding to the level at which perfusion CT was performed.

Quantification of MVD was performed after immunostaining with a CD34 monoclonal antibody (QBEnd/10, MAB-0034; Fujian Maixin Biotechnology Company, China), which was according to Weidner's revised technique [6] (Fig. 2). The whole slide was viewed at

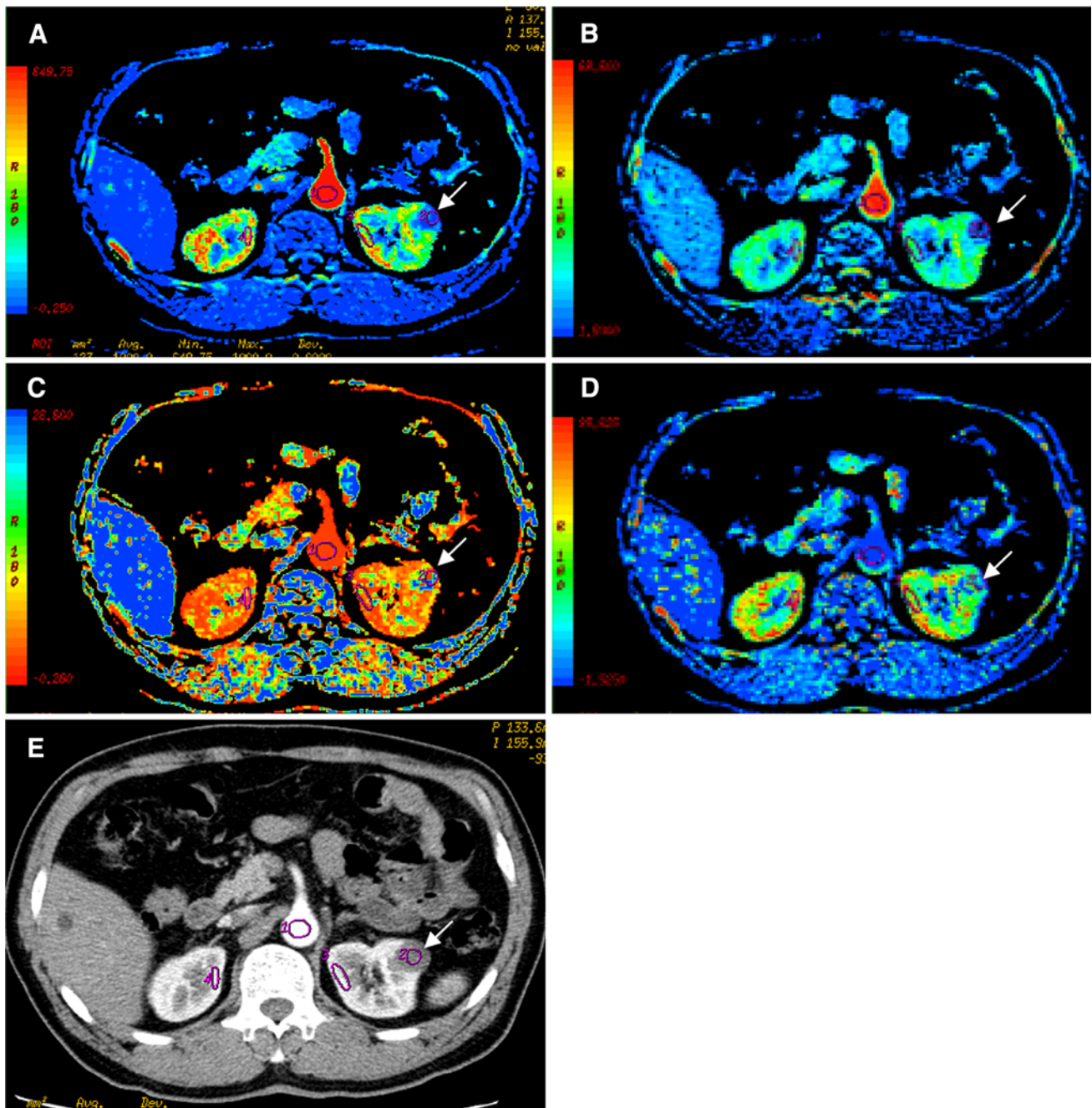


Fig. 1. Parametric maps (A–D) and corresponding morphologic CT imaging (E) show there are difference in blood flow (A), blood volume (B), mean transit time (C), and per-

meability surface-area product (D) between renal cell carcinoma (arrow) and normal renal cortex (color figure online).

100× FOV under the microscope, and the “hotspot” (the most intensive area of tumor angiogenesis) was found. Then under the 400× FOV, the number of tumor vessels in six random areas was counted and averaged as MVD count.

Semiquantification of VEGF expression was performed after immunostaining with a VEGF monoclonal antibody (ST28, ZA-0509; Beijing Zhongshan Golden Bridge Biotechnology Limited Corporation, China)

(Fig. 3). Four groups were formed according to staining intensity and the percentage of positive carcinoma cells with cytoplasmic staining: negative (0) <5%, weak positive (+1) 5–25%, moderate positive (+2) 26–50% and intense positive (+3) >51%.

Two pathologists counted MVD, respectively, and mean values were calculated and recorded for each patient. VEGF expression was assessed by the two pathologists through discussion.

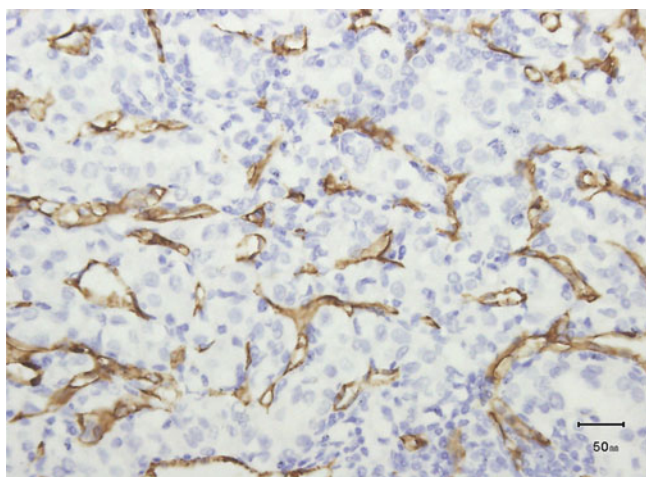


Fig. 2. CD34 stain (original magnification 400 \times). The vessels stained positively appear *brown* (color figure online).

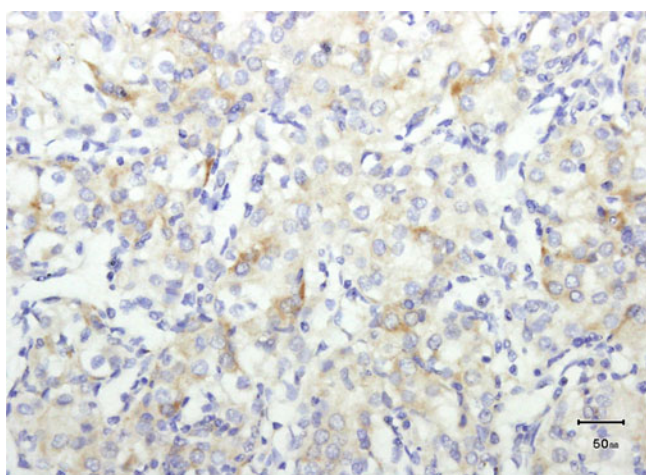


Fig. 3. VEGF stain (original magnification 400 \times). Carcinoma cells stained positively appear *brown* in the cytoplasm (color figure online).

Statistical analysis

All statistical analyses were performed by using a statistical software (SPSS 13.0 for Windows). The mean values (with standard deviations) of MVD and all perfusion parameters were calculated. Two-tailed student *t*-test was used to compare perfusion parameters between normal renal cortex and RCC. One-way ANOVA was used to analyze statistical difference of MVD counts, level of VEGF expression and all perfusion parameters in the different subtypes of RCC. Pearson correlation coefficient analysis was performed to determine if there were any linear associations between the perfusion CT parameters and MVD count. Spearman rank correlation analysis was performed to assess the relationships between each perfusion CT parameters and VEGF expression. Statistical significance was assigned at the 5% level.

Results

Mean perfusion CT parameter (blood flow, blood volume, mean transit time, and permeability surface-area product) of normal renal cortex and RCC values are summarized in Table 1. There were significant difference in all the four perfusion parameters between normal renal cortex and RCC ($P < 0.01$) (Fig. 1).

Histologic parameter (MVD, VEGF) values of 73 cases RCC are shown in Table 2.

Perfusion CT and histologic parameters of RCC histologic subtypes are summarized in Table 3. MVD, BF and BV among subtypes of RCC were significantly different ($P < 0.05$). There were not significant difference in VEGF expression, MTT, and PS among all the subtypes.

MVD, BF, BV, and MTT between clear cell RCC and papillary RCC were statistically different (Table 4). Mean values of MVD, BF, and BV were significantly higher in clear cell RCC than in papillary RCC ($P < 0.05$). And mean MTT was lower in clear cell RCC than in papillary RCC ($P = 0.015$). No difference was found between the perfusion parameters of clear cell RCC and chromophobe RCC, neither between papillary RCC and chromophobe RCC.

BV, BF and PS measurements of RCC correlated positively with MVD, but MTT did not (Table 5). No significant association between any perfusion CT parameter of RCC and VEGF expression was observed (Table 5).

Discussion

Perfusion CT parameters of normal tissues have been reported in some studies previously [3, 7, 8]. However, to our knowledge, there is no report about the perfusion parameters of kidney. In our study, we showed the perfusion CT parameters of normal renal parenchyma, including BF, BV, MTT, and PS. We also found there was significant difference between the normal renal cortex and renal cell carcinoma in all mean values of these parameters. Thus, perfusion CT is a feasible technique to assess tissue perfusion in patients with renal cell carcinoma.

The 2004 World Health Organization classification for renal neoplasms recognizes several distinct histologic subtypes of RCC, including clear cell RCC, papillary RCC, chromophobe RCC, multilocular cystic RCC, collecting duct carcinoma, medullary carcinoma, and so on. Distinct histologic subtypes of RCC have characteristic histomorphologic and biologic profiles. Clear cell RCC is the most common subtype and has a less favorable prognosis (stage for stage) than do papillary RCC and chromophobe RCC. Collecting duct carcinoma and renal medullary carcinoma are associated with aggressive clinical behavior and a poor prognosis.

Table 1. Perfusion CT parameter values for kidney

	Normal renal cortex (mean \pm SD)	Renal cell carcinoma (mean \pm SD)	<i>t</i> Value	<i>P</i> value
BF (mL/min/100 g)	454.32 \pm 110.90	261.96 \pm 175.86	-7.620	0.000
BV (mL/100 g)	23.53 \pm 5.71	17.17 \pm 8.34	-5.193	0.000
MTT (s)	3.62 \pm 1.38	7.08 \pm 3.42	7.670	0.000
PS (mL/min/100 g)	63.95 \pm 18.85	25.07 \pm 13.20	-14.193	0.000

Table 2. Histologic parameter values for 73 cases RCC

Histologic parameter	Value
MVD (mean \pm SD)	42.29 \pm 21.00
VEGF (<i>n</i> , %)	
0	35, 47.9%
+1	24, 32.9%
+2	10, 13.7%
+3	4, 5.5%

Accurate subtyping of RCC by using imaging modality is critical for designing optimal treatment protocols for patients and predicting prognosis. Conventional CT imaging features of common and uncommon histologic subtypes of RCC were summarized by Prasad [9], and they have characteristic features, respectively. Our results showed mean values of BF, BV were significantly higher and mean MTT was significantly lower in clear cell RCC than in papillary RCC ($P < 0.05$). So perfusion CT can also reveal the different characteristic of RCC histologic subtypes according to the quantitative information.

MVD is a potential prognostic factor that has been correlated with clinical stage, pathologic stage, metastasis, and histopathologic grade, and is a significant predictor of disease-specific survival and progression after therapy [2, 10]. The correlation between MVD and the perfusion CT parameters has been previously analyzed in colorectal carcinoma, and the results were inconsistent

[5, 11]. Positive correlations between CT parameters and MVD have been reported in studies of lung cancer and pancreatic endocrine tumors [3, 12, 13]. In our study, we found a significant correlation between MVD and BF, BV, and PS, respectively. It is consistent with the reported results of other studies: Wang [14] showed all the enhancement parameters (ΔH , TBR, AR, and slope) of dynamic CT in RCC correlated with MVD; Kaneoya [15] analyzed the functional CT imagines of 14 RCCs, and found there were significant linear correlation between functional CT parameters (relative blood volume, permeability 1, and permeability 2) and MVD. Compared with the analysis previously reported, the perfusion CT technique we utilized provided a more accessible assessment of tissue perfusion with four perfusion CT parameters (BF, BV, MTT, and PS).

VEGF is thought to play a major role in tumor angiogenesis. A few perfusion CT studies in which investigators have attempted to assess angiogenesis have revealed conflicting results. Goh [5] found there was not significant association between any perfusion CT parameter and VEGF score in colorectal cancer. Yet Ma [16] reported that the peripheral lung cancers with VEGF positive expression showed significantly higher PH, PHpm/PHa, BF, BV, and PS value than those of the peripheral lung cancer with VEGF negative expression. Zhang [17] showed there was a good positive correlation between BF, BV, PS and VEGF, and negative between

Table 3. Perfusion CT and histologic parameters of RCC subtypes

	MVD (mean \pm SD)	VEGF (no. of cases)				BF (mean \pm SD)	BV (mean \pm SD)	MTT (mean \pm SD)	PS (mean \pm SD)
		0	+1	+2	+3				
Clear cell (<i>n</i> = 65)	44.79 \pm 20.05	31	22	9	3	279.61 \pm 177.02	17.97 \pm 8.30	6.85 \pm 3.39	25.78 \pm 12.94
Papillary (<i>n</i> = 3)	9.63 \pm 2.55	0	2	0	1	52.00 \pm 51.77	4.82 \pm 2.93	11.74 \pm 3.63	11.90 \pm 5.12
Chromophobe (<i>n</i> = 5)	29.32 \pm 19.87	4	0	1	0	158.49 \pm 49.79	14.22 \pm 3.21	7.26 \pm 1.77	23.69 \pm 17.41
<i>F</i> value	5.699	2.020				3.568	4.257	3.106	1.642
<i>P</i> value	0.005	0.140				0.033	0.018	0.051	0.201

Table 4. Comparison among the perfusion parameters and histologic parameters of RCC subtypes

	MVD	VEGF	BF	BV	MTT	PS
Clear cell and papillary	0.004	0.083	0.026	0.007	0.015	0.077
Clear cell and chromophobe	0.096	0.388	0.129	0.315	0.793	0.732
Papillary and chromophobe	0.177	0.052	0.394	0.112	0.069	0.221

Data is the *P* value

Table 5. Correlation between perfusion parameters and histologic parameters of RCC

	BF		BV		MTT		PS	
	<i>r</i> Value	<i>P</i> value	<i>r</i> Value	<i>P</i> value	<i>r</i> Value	<i>P</i> value	<i>r</i> Value	<i>P</i> value
MVD	0.283	0.015	0.381	0.001	-0.210	0.074	0.319	0.006
VEGF	-0.076	0.523	-0.132	0.267	0.009	0.940	-0.197	0.094

MTT and VEGF in rabbit VX2 soft-tissue tumor. About RCC, Kaneoya [15] reported the significant correlation between VEGF grade and permeability 2, but no correlation was found between all the perfusion CT parameters and VEGF expression in our study. Clearly, the relationship between VEGF expression and functional tumor vascularity is complex. To date, there has been no enough evidence suggesting that VEGF expression may be replaced by quantitative perfusion CT parameters.

Antiangiogenesis has become the new strategy for treating tumor because of its evident effectiveness in constraining tumor growth [18–20]. Several antiangiogenic therapies for RCC have shown promise in pre-clinical studies and are currently being evaluated in clinical trials [21–24]. It has become a challenging goal for the radiologist to assess noninvasively the physiology of tumor microcirculation, in addition to conventional morphology. A few studies about assessing effect of antiangiogenesis therapy with functional CT imaging were reported. Koukourakis [25] found that the “perfusion score” of colorectal carcinoma significantly decreased after the administration of bevacizumab. Kan [26] reported some perfusion CT parameters were significantly differentiated between treated tumors and control tumors in a rat model. Another investigation in a rabbit model showed the perfusion parameters after interventional therapy were significant different with values of pre-therapy [17]. Some studies showed functional MRI parameters change after antiangiogenic therapy correlated with clinical outcome in metastatic RCC [27, 28]. Evaluating antiangiogenic therapy for RCC with functional CT has not been reported.

Whereas conventional CT can only depict morphologic characters of tumor, perfusion CT can provide additional quantitative preoperative prognostic factors that could influence therapeutic treatment of patients [3, 29]. Otherwise, the efficacy of antiangiogenesis is known to be correlated with the degree of angiogenesis. The more angiogenesis a tumor has, the more effective antiangiogenesis is. So perfusion CT is helpful to plan treatment and determine if the antiangiogenesis therapy is necessary.

Magnetic resonance imaging (MRI), positron emission tomography (PET) and computer tomography (CT) have been used to assess tumor angiogenesis in vivo [18, 30]. Dynamic contrast enhanced multislice CT is commonly used method for this kind of diagnosis. An important advantage of CT over other imaging modalities

is that the contrast enhancement is linearly proportional to the concentration of contrast medium in the tissues, which is advantageous for quantitative assessment in pharmacokinetic analysis. The higher temporal and spatial resolution is another major advantage, which is essential for monitoring the detailed time-course change of enhancement and identifying anatomical structures accurately. However, a major disadvantage is the radiation exposure for patients. Anyway, perfusion CT is becoming possible to gain functional information by using this emerging and promising approach.

Our study had a number of limitations. First, perfusion CT findings in histologic subtypes of RCC were analyzed in our study, but the number of cases of non-clear cell RCC was insufficient, so further studies are needed. Although the supervising radiologist and pathologist took care specially, the exact matching histopathologic slice to imaging slice was very difficult. The inevitable mismatch between the histopathologic specimen and the CT finding has an impact on the degree of correlation. Long-term follow-up in patients has not been performed to assess direct prognostic value of perfusion parameters. Further studies are needed to address this point.

On the other hand, the perfusion CT examination conferred an additional effective dose and required additional volume of intravenous contrast medium to be administered.

In conclusion, we show that perfusion CT is feasible in patients with renal cell carcinoma and allows evaluation of tumor angiogenesis. By providing an in vivo marker of angiogenesis, perfusion CT is becoming widely used for the diagnosis and predicting prognosis of renal cell carcinoma and for the monitoring of its response to antiangiogenesis therapy.

References

1. Cuenod CA, Fournier L, Balvay D, et al. (2006) Tumor angiogenesis: pathophysiology and implications for contrast-enhanced MRI and CT assessment. *Abdom Imaging* 31:188–193
2. Lzawa J, Dinney CPN (2001) The role of angiogenesis in prostate and other urologic cancers: a review. *Can Med Assoc J* 164:662–670
3. d’Assignies G, Couvelard A, Bahrami S, et al. (2009) Pancreatic endocrine tumors: tumor blood flow assessed with perfusion CT reflects angiogenesis and correlates with prognostic factors. *Radiology* 250:407–416
4. Yi CA, Lee KS, Kim EA, et al. (2004) Solitary pulmonary nodules: dynamic enhanced multi-detector row CT study and comparison with vascular endothelial growth factor and microvessel density. *Radiology* 233:191–199
5. Goh V, Halligan S, Daley F, et al. (2008) Colorectal tumor vascularity: quantitative assessment with multidetector CT—do tumor

- perfusion measurements reflect angiogenesis? *Radiology* 249:510–517
6. Weidner N (1995) Intratumor microvessel density as a prognostic factor in cancer. *Am J Pathol* 147:9–19
 7. Xue HD, Jin ZY, Liu W, et al. (2006) Perfusion characteristics of normal pancreas and insulinoma on multi-slice spiral CT. *Zhongguo Yi Xue Ke Xue Yuan Xue Bao* 28:68–70
 8. Galvez M, York GE II, Eastwood JD (2004) CT perfusion parameter values in regions of diffusion abnormalities. *Am J Neuroradiol* 25:1205–1210
 9. Prasad SR, Humphrey PA, Catena JR, et al. (2006) Common and uncommon histologic subtypes of renal cell carcinoma: imaging spectrum with pathologic correlation. *Radiographics* 26:1795–1810
 10. Yildiz E, Ayan S, Goze F, et al. (2008) Relation of microvessel density with microvascular invasion, metastasis and prognosis in renal cell carcinoma. *BJU Int* 101:758–764
 11. Li ZP, Meng QF, Sun CH, et al. (2005) Tumor angiogenesis and dynamic CT in colorectal carcinoma: radiologic–pathologic correlation. *World J Gastroenterol* 11(9):1287–1291
 12. Li Y, Yang ZG, Chen TW, et al. (2008) Peripheral lung carcinoma: correlation of angiogenesis and first-pass perfusion parameters of 64-detector row CT. *Lung Cancer* 61:44–53
 13. Ma SH, Xu K, Xiao ZW, et al. (2007) Peripheral lung cancer: relationship between multi-slice spiral CT perfusion imaging and tumor angiogenesis and cyclin D1 expression. *Clin Imaging* 31:165–177
 14. Wang JH, Min PQ, Wang PJ, et al. (2006) Dynamic CT evaluation of tumor vascularity in renal cell carcinoma. *AJR* 186:1423–1430
 15. Kaneoya K, Ueda T, Suito H, et al. (2008) Functional computed tomography imaging of tumor-induced angiogenesis: preliminary results of new tracer kinetic modeling using a computer discretization approach. *Radiat Med* 26:213–221
 16. Ma SH, Le HB, Jia BH, et al. (2008) Peripheral pulmonary nodules: relationship between multi-slice spiral CT perfusion imaging and tumor angiogenesis and VEGF expression. *BMC Cancer* 8:186
 17. Zhang J, Wang R, Lou H, et al. (2008) Functional computed tomographic quantification of angiogenesis in rabbit VX2 soft-tissue tumor before and after interventional therapy. *J Comput Assist Tomogr* 32:697–705
 18. Passe TJ, Bluemke DA, Siegelman SS (1997) Tumor angiogenesis: tutorial on implications for imaging. *Radiology* 203:593–600
 19. Connolly DT, Heuvelman DM, Nelson R, et al. (1989) Tumor vascular permeability factor stimulates endothelial cell growth and angiogenesis. *J Clin Invest* 84:1470–1478
 20. Folkman J (1971) Tumor angiogenesis: therapeutic implications. *N Engl J Med* 258:1182–1186
 21. Dhanabal M, Ramchandran R, Volk R, et al. (1999) Endostatin: yeast production, mutants, and antitumor effect in renal cell carcinoma. *Cancer Res* 59:189–197
 22. Morita T, Shinohara N, Tokue A (1994) Antitumor effect of a synthetic analogue of fumagillin on murine renal carcinoma. *Br J Urol* 74:416–421
 23. Fujioka T, Hasegawa M, Ogino K, et al. (1996) Antitumor effects of angiogenesis inhibitor 0-(choroacetyl-carbamoyl) fumagillol (TNP-470) against murine renal carcinoma. *J Urol* 155:1775–1778
 24. Stadler WM, Kuzel T, Shapiro C, et al. (1999) Multi-institutional study of the angiogenesis inhibitor TNP-470 in metastatic renal carcinoma. *J Clin Oncol* 17:2541–2545
 25. Koukourakis MI, Mavani I, Kouklakis G, et al. (2007) Early antivascular effects of bevacizumab anti-VEGF monoclonal antibody on colorectal carcinomas assessed with functional CT imaging. *Am J Clin Oncol* 30:315–318
 26. Kan Z, Phongkitkarun S, Kobayashi S, et al. (2005) Functional CT for quantifying tumor perfusion in antiangiogenic therapy in a rat model. *Radiology* 237:151–158
 27. de Bazelaire C, Alsop DC, George D, et al. (2008) Magnetic resonance imaging-measured blood flow change after antiangiogenic therapy with PTK787/ZK 222584 correlates with clinical outcome in metastatic renal cell carcinoma. *Clin Cancer Res* 14:5548–5554
 28. Flaherty KT, Rosen MA, Heitjan DF, et al. (2008) Pilot study of DCE-MRI to predict progression-free survival with sorafenib therapy in renal cell carcinoma. *Cancer Biol Ther* 7:496–501
 29. Makari Y, Yasuda T, Doki Y, et al. (2007) Correlation between tumor blood flow assessed by perfusion CT and effect of neoadjuvant therapy in advanced esophageal cancers. *J Surg Oncol* 96:220–229
 30. McDonald DM, Choyke PL (2003) Imaging of angiogenesis: from microscope to clinic. *Nat Med* 9:713–725